Coupled Magneto-Thermal Model for an Encapsulated Busbars System Using QuickField

Ioan C. Popa and Alin-Iulian Dolan

University of Craiova, Faculty of Electrical Engineering
Craiova, Romania
e-mail: ipopa@elth.ucv.ro, adolan@elth.ucv.ro

Abstract— In this paper, we propose an approach for the magnetic and thermal modeling of an encapsulated busbars system, in three-phase execution, for high voltage using QuickField software. The paper proposes a numerical model developed by coupling of the magnetic field problem with the stationary and transient heat field problems for the geometry of a three-phase execution busbars system with common shield. The coupling of problems is realized by importing specific losses from the magnetic field problem as heat sources for thermal field problem. The magnetic field problem is also coupled to the electrical circuit. The electrodynamic forces that occur between conductors in the presence of the ferromagnetic shield have different values compared to those that occur in an unshielded system. In the model it was taken into account the variation of electrical conductivity with the temperature. The global heat transfer coefficient by convection and radiation used in thermal model was estimated using the power losses computed by magnetic model. When evaluating the global heat transfer coefficient was taken into account the temperature dependence of the physical properties of the air. There is a good agreement between numerical and analytical temperature values. The paper analyzes the results for two materials used to build the shield, iron and aluminum. The presented model can be used for analysis, design and optimization of three-phase busbars system with common shield.

I. INTRODUCTION

The shielded busbars systems are used to establish the connection between the generator and the transformer in a power plant.

There are two types of construction [1], [2], [7]:
- Single phase execution with short-circuited shields at both ends and connected to ground [7] or with interrupted by segments shield and connected to ground;
- Three-phase execution, with a common grounded shield (Fig. 1).

For the single phase execution, the active conductor (of aluminum) is placed in a metal grounded shield (also of aluminum). For the three-phase execution all the active conductors are arranged in a common grounded shield (of iron or aluminum). Internal insulation (between the active conductor and the shield) is performed in air at normal pressure or with SF6 gas at a pressure of 3 - 5 bars.

The single-phase execution is used when we have a small distances between generator and transformer. The three-phase execution is used at greater distances between

generator and transformer, when the overall dimensions are important [15].

The construction of shielded busbars must meet the following requirements:
- The elimination of the ability to produce accidental short circuits (insulation pollution etc.).
- The elimination of the possibility of accidental electrocution by touching the bars under tension;
- The low annual costs (return of investments and the Joule losses in the shields);
- Reduction of electrodynamics forces.
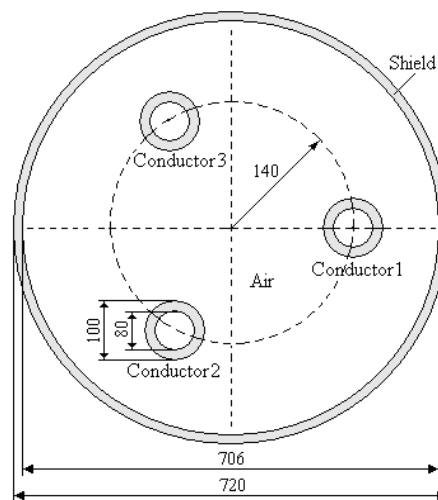
Fig. 1. Geometry of three phase busbars system with common shield.

If the shields are short-circuited and grounded at both ends then they produce a circulation of currents approximately equals and in opposite phase with corresponding currents of active conductors [1], [7]. This construction involves a close to zero magnetic field outside the shield and therefore the electrodynamic forces acting between phases are close to zero. This is one of the advantages of this technical solution, but a disadvantage is represented by the Joule losses in the shield.

In the case of common shield, the electrodynamic forces between conductors at short-circuit current take great values, but these are different compared to the case of absence of the shield. The results show that this difference is not large, so that the electrodynamic forces can be analytically calculated neglecting this shield.

II. MODEL EQUATIONS

A. Magnetic Field Equation

The governing equation for AC magnetics analysis for rated and short-circuit currents is

$$\frac{\partial}{\partial x}\left(\frac{1}{\mu}\frac{\partial A}{\partial x}\right)+\frac{\partial}{\partial y}\left(\frac{1}{\mu}\frac{\partial A}{\partial y}\right)-\sigma\frac{\partial A}{\partial t}=-J_s \qquad (1)$$

where A is the magnetic potential vector, μ is the permeability, σ is the electrical conductivity and J_s is the source current density. In Fig. 2 is presented the electric circuit model.

B. Heat Transfer Equations

In steady-state regime the thermal governing equation is

$$\frac{\partial}{\partial x}\left(\lambda\frac{\partial T}{\partial x}\right)+\frac{\partial}{\partial y}\left(\lambda\frac{\partial T}{\partial y}\right)+S=0 \qquad (2)$$

where T is the temperature, λ is the thermal conductivity and S is the source term (power losses in conductors and shield).

In transient regime the thermal governing equation is

$$\frac{\partial}{\partial x}\left(\lambda\frac{\partial T}{\partial x}\right)+\frac{\partial}{\partial y}\left(\lambda\frac{\partial T}{\partial y}\right)+S=\rho c_p\frac{\partial T}{\partial t} \qquad (3)$$

where ρ is the mass density and c_p is specific heat. The heat transfer mechanism in busbar is done in Fig. 3.

C. Shield temperature

The global thermal transmissivity is [1], [2], [7], [14]

$$\alpha = M(T_2 - T_{ma})^{0.2}. \qquad (4)$$

$$M = 2.65 K_B \varepsilon T_{ma}^3 + 0.9\left(\frac{\lambda^4 c_p \rho^2 \beta g}{\mu d_c^3}\right)^{0.2} \qquad (5)$$

where K_B – Boltzmann constant, ε - shield emissivity, λ - air thermal conductivity, c_p – air specific heat capacity, ρ - air density, β - volumetric expansion coefficient, g - gravitational acceleration, μ - dynamic viscosity, d_c - characteristic dimension (the outer diameter of the shield).

The specific thermal flux from shield to environment is

$$P_e = \frac{P_1 + P_2}{A} = \frac{P_1 + P_2}{\pi D} = \alpha\Delta T \qquad (6)$$

where A is exterior surface shield area per length unity, D is outer shield diameter and $\Delta T = T_2 - T_{ma}$.

From (4) and (6) results the global thermal transmissivity
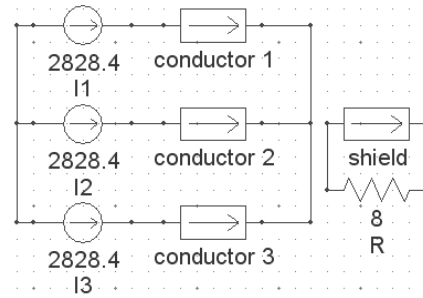
Fig. 2. Electric circuit model for rated current (I_n = 2000 A) in QuickField.
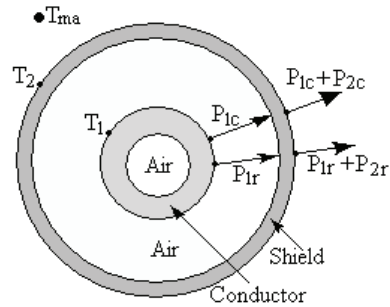
Fig. 3. Heat transfer mechanism of a single-phase busbar.

$$\alpha = \left(M P_e^{0.2}\right)^{1/1.2} \qquad (7)$$

The over-temperature and the temperature of the shield are

$$\Delta T = \frac{P_e}{\alpha}, \qquad T_2 = T_{ma} + \Delta T \qquad (8)$$

D. Conductor temperature

To determine the active conductor temperature is calculated both heat flux transferred by conduction and convection and heat flux transferred by radiation.

The heat flux transferred by convection and conduction from the active conductor to shield is approximated by the relationship [7]

$$P_{1c} = (T_1 - T_2)^{1.2} \cdot 2\pi\lambda \cdot 0.4\left(\frac{\rho(r_2 - r_1)^3}{\mu}Pr\right)^{0.2} \cdot 1/\ln\left(\frac{r_2}{r_1}\right) \quad (9)$$

where r_1 - radius arrangement of conductors centers, r_2 - inner radius of the shield and the parameters λ, ρ, μ and Pr (Prandtl number) concern the gas between active conductor and shield. The difference $r_2 - r_1$ is considered the characteristic dimension in this case. The relationship (9) can be written

$$P_{1c} = b(T_1 - T_2)^{1.2} \qquad (10)$$

$$b = 2\pi\lambda \cdot 0.4\left(\frac{\rho(r_2 - r_1)^3}{\mu}Pr\right)^{0.2} \cdot 1/\ln\left(\frac{r_2}{r_1}\right) \qquad (11)$$

The thermal flux transferred by radiation from active conductor to shield is calculated by relationship

$$P_{1r} = c\left(T_1^4 - T_2^4\right) \qquad (12)$$

$$c = 2\pi r_1 K_B \Big/ \left(\frac{1}{\varepsilon_1} + \left(\frac{1}{\varepsilon_2} - 1\right)\frac{r_1}{r_2}\right) \qquad (13)$$

Adding the two thermal flux, from (10) and (12) results

$$b(T_1 - T_2)^{1.2} + c(T_1^4 - T_2^4) = P_1 \qquad (14)$$

where the coefficients b and c are known (from (11) and (13)) and T_2 is absolute shield temperature and it is known. The total thermal flux P_1 is computed by AC Magnetic model (table I).

Based on relations (4) - (14), a program have been developed to compute the global heat transfer coefficients for shield and for conductor and the temperatures of the shield T_2 and of the conductor T_1.

The conductor temperature T_1 is done by solving of (14).

E. Heat transfer coefficient

The global heat transfer coefficient α depends on the physical properties of air (thermal conductivity λ, specific heat c_p, dynamic viscosity μ, air density ρ), on the quality of surface (emissivity ε) and on the surface temperature of the shield/conductor (in fact, on the difference of temperature between conductor/shield and environment). On the other hand, the physical properties depend on the temperature of the air. Thus, in order to take into account for this dependence, the following analytical relationships [11], valid in the temperature range 200-400 K, were used

$$\rho(T) = \frac{351.99}{T} + \frac{344.84}{T^2} \quad \left[\frac{\text{kg}}{\text{m}^3}\right] \qquad (15)$$

$$\mu(T) = \frac{1.4592\,T^{3/2}}{109.1 + T} \quad \left[10^{-6}\,\frac{\text{N}\cdot\text{s}}{\text{m}^2}\right] \qquad (16)$$

$$\lambda(T) = \frac{2.334\cdot10^{-3}\,T^{3/2}}{164.54 + T} \quad \left[\frac{\text{W}}{\text{mK}}\right] \qquad (17)$$

$$c_p(T) = 1030.5 - 0.19975\,T + 3.9734\cdot10^{-4}\,T^2 \qquad (18)$$

where T is absolute temperature absolute in Kelvin.

Figure 4 shows the variation of global heat transfer coefficient depending on the emissivity for the conductor and shield considering the variation of the physical properties of the air with the temperature.

Figure 5 shows the shield temperature variation depending on the emissivity.

Figures 6 and 7 shows the variation of global heat transfer coefficient for conductor and shield depending on the difference of temperature for different values of emissivity and for ambient temperature of 40 $^{\text{o}}$C.

F. Analytical results

With the next values of quantities in equations (4) – (14): $\theta_{ma} = 40°C$, $\lambda = 0.027$ Wm^{-1}K^{-1}, $\varepsilon = 0.6$, $\beta = 0.003194$, $c_p = 1010$ J·kg^{-1}K^{-1}, $\rho = 1.128$ kg·m^{-3}, $d_c = 0.72$ m (for shield), $d_c = 0.213$ m (for conductor) $P_1 = 43.75$ W/m, $P_2 = 19.93$ W/m, $\varepsilon_1 = \varepsilon_2 = 0.9$, $r_1 = 0.14$ m, $r_2 = 0.353$ m, $P_r = 0.71$, results the global heat transfer coefficient for shield $\alpha_2 = 6.54$ Wm^{-2}K^{-1}, shield temperature $\theta_2 = 54.79$ °C, the global heat transfer coefficient for conductor $\alpha_1 = 8.25$ Wm^{-2}K^{-1} and temperature $\theta_1 = 74.4$ °C.

In Fig. 8 is presented the block diagram of coupled problems in QuickField software. The magnetic problems are also connected with electric circuit problem.
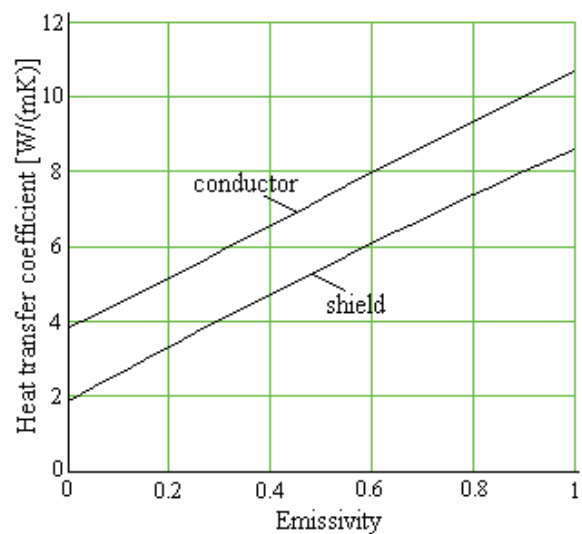
Fig. 4. Heat transfer coefficient versus emissivity for conductor and shield.
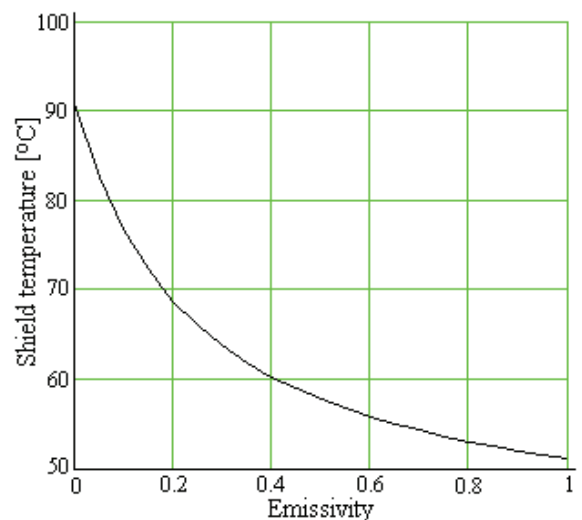
Fig. 5. Shield temperature versus emissivity.
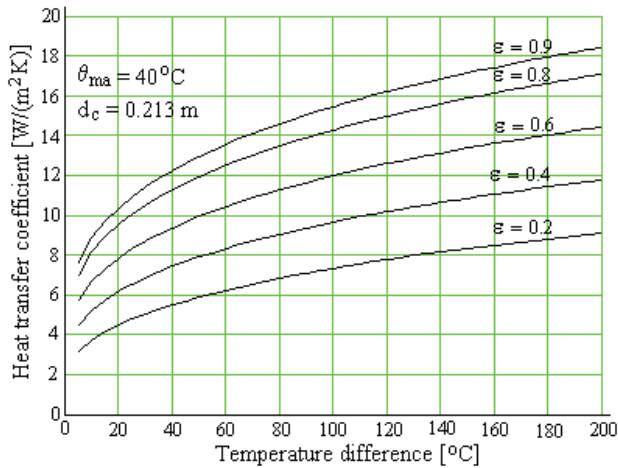
Fig. 6. Heat transfer coefficient versus temperature difference (at different emissivities) for conductor.
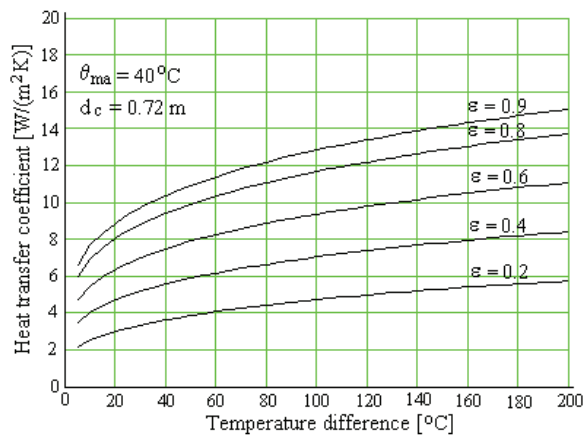
Fig. 7. Heat transfer coefficient versus temperature difference (at different emissivities) for shield.

Fig. 8. Coupled problems model for transient thermal analysis for short-circuit current (I_t = 40 kA).
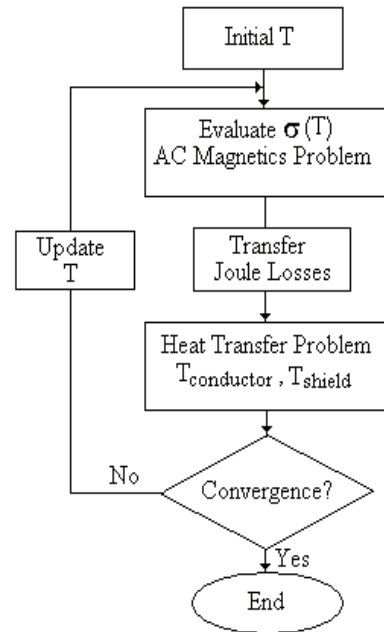
Fig. 9. Coupled analysis procedure of magnetic and thermal field in QuickField.

In Fig. 9 is presented the block diagram of coupled analysis procedure of magnetic and thermal field, to update the electric conductivity in QuickField software.

G. Electrodynamic forces

The analytic computation of electrodynamic forces in stabilizing short-circuit (Fig. 6) can be achieved, in a first approximation, neglecting the shield and the tubular conductor can be approximated by an equivalent full cylindrical conductor.

Thus, the resulting electrodynamic force acting on conductor 1 and its components are [7]

$$F_1(t) = \sqrt{F_x^2(t) + F_y^2(t)} \qquad (19)$$

$$F_x(t) = \frac{\sqrt{3}}{2} CI^2\left(1 - \cos 2\omega t\right), F_y(t) = \frac{\sqrt{3}}{2} CI^2 \sin 2\omega t \quad (20)$$

where I is the RMS value of short-circuit current and C is the contour coefficient ($C = 10^{-7} \cdot 2l/a$, $l = 1 m$, $a = r_1\sqrt{3}$ being distance between the conductor axis). The contour coefficient was corrected taking into account the

nonfiliform and finite length ($\varphi_c = a/(a-r)$, r being the conductor radius).

The contour coefficient was corrected taking into account the nonfiliform and finite length ($\varphi_c = a/(a-r)$, r being the conductor radius).

The maximum force in stabilizing short-circuit regime is

$$F_{1\max} = \sqrt{3}CI^2 \qquad (21)$$

The maximum force in transient short-circuit regime, in a standard network, having the shock factor k_y =1.8, is

$$F_{1\max tr} = \sqrt{3}Ck_y^2 I^2 \qquad .(22)$$

Time variation of force (according to (19)) is shown in Fig. 10. The results provided by the numerical model show that the presence of the ferromagnetic shield reduces electrodynamic forces by 4.24 %.

In the case of shield on aluminum is found that the average value of force acting on a conductor is reduced by 50% compared to the case of the absence of the shield.

The same value is 47.8% lower compared to the shield on iron.
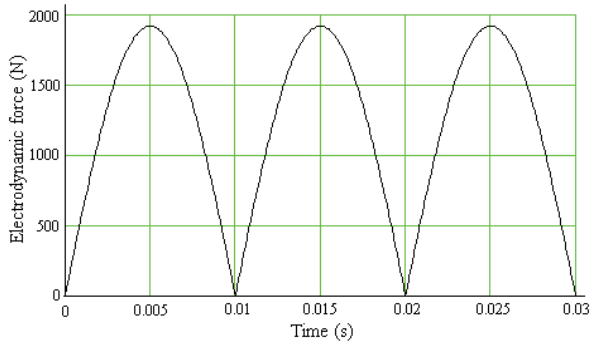
Fig. 10. Time variation of electrodynamic force negleting shield
(I = 40 kA, $F_{average.}$ = 1223 N, F_{max} = 1920.3 N)

The error between electrodynamic force analytically calculated (neglecting the shield) and the values resulting from the numerical model is 3.56 %.

III.   NUMERICAL RESULTS

The Fig. 11 - 12 shows the magnetic flux density and temperature distribution for busbars system geometry, at rated current, with the dimensions presented in Fig.1. In table I different physical quantities are presented for shield built in iron and aluminum (the results for aluminum are marked by *). In table II is presented different physical quantities in busbars system at short-circuit regime for shield built in iron and aluminum.

Table III shows a comparison of the temperatures for the conductor and shield at rated current, calculated analytically and numerically.

It finds an error of 11-13 % can be explained on the one hand by the fact that in the numerical model the iterations for adjusting the value of heat transfer coefficient were not automatically. On the other hand, the characteristic dimension of conductor was considered the difference r_2 - r_1 that has not a very precise justification. The IEC – 517 standard stipulates the maximum values of 65 °C for overtemperature for conductor and of 30 °C for shield.

Table IV shows the evolution of temperature for conductor and shield in short-circuit regime.

The presented numerical model and analytical method were validated experimentally for a system of single-phase busbar execution [2].

It is found that the Joule losses in conductors are smaller in shielded than unshielded conductors and smaller by 5.4% for aluminum than iron shield, in short-circuit regime.

φ = 0°   φ = 120°

φ = 240°   Detail for conductor 3
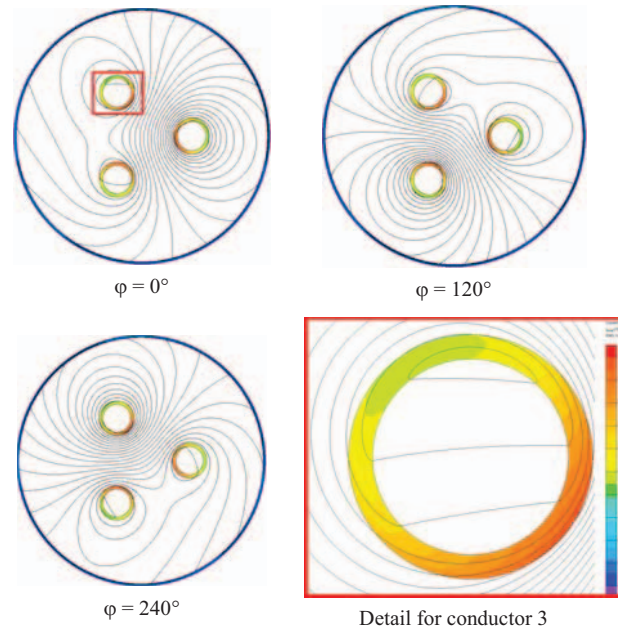
Fig. 11. Magnetic flux density lines and current density distributions.
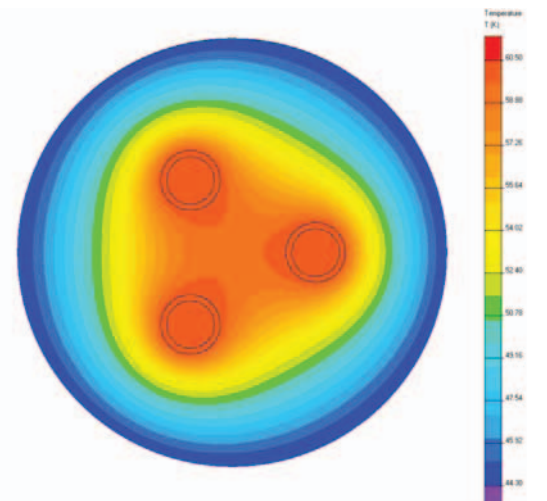
Fig. 12. Thermal field distribution in busbars for rated current (I_n = 2000 A).

The Table I shows that at rated current, the Joule losses in conductors are smaller by 9.3% for aluminum than iron shield. In the same regime, the losses in shield are smaller by 80.1% for aluminum than iron and in short-circuit, these decrease by 81.5%.

TABLE I. PHYSICAL QUANTITIES IN BUSBARS SYSTEM AT RATED CURRENT (I_n = 2000 A, RMS VALUE)

	Conductor 1	Conductor 2	Conductor 3	Shield
Joule heat [W/m]	54.794 49.684 *	54.794 49.684 *	54.794 49.684 *	64.223 11.51 *
Total current (peak value) [A]	2828.4	2828.4	2828.4	0.009257
Total inductance [H/m]	$3.12 \cdot 10^{-7}$ $2.757 \ 10^{-7}$ *	$3.12 \cdot 10^{-7}$ $2.757 \ 10^{-7}$ *	$3.12 \cdot 10^{-7}$ $2.757 \ 10^{-7}$ *	$2.046 \ 10^{-7}$ $3.799 \ 10^{-7}$ *
Impedance [Ω/m]	$9.984 \cdot 10^{-5}$ $8.761 \ 10^{-5}$ *	$9.984 \cdot 10^{-5}$ $8.761 \ 10^{-5}$ *	$9.984 \cdot 10^{-5}$ $8.761 \ 10^{-5}$ *	0.000115 $1.181 \ 10^{-4}$ *
Resistance [Ω/m]	$1.905 \cdot 10^{-5}$	$1.905 \cdot 10^{-5}$	$1.905 \cdot 10^{-5}$	$9.531 \ 10^{-5}$

	$1.319 \ 10^{-5}$ *	$1.319 \ 10^{-5}$ *	$1.319 \ 10^{-5}$ *	-
Reactance [Ω/m]	$9.801 \cdot 10^{-5}$	$0.98 \cdot 10^{-4}$	$9.988 \cdot 10^{-5}$	$6.428 \ 10^{-5}$
	$8.661 \ 10^{-7}$ *	$8.661 \ 10^{-7}$ *	$8.661 \ 10^{-7}$ *	-
Skin effect coefficient ($k_s = R_{AC}/R_{DC}$)	1.151	1.151	1.151	
Voltage drop [mV/m]	282.39	282.38	282.38	$1064.3 \ 10^{-6}$
	247.8 *	247.79 *	247.79 *	$3789.6 \ 10^{-7}$ *

TABLE II. PHYSICAL QUANTITIES IN BUSBARS SYSTEM AT SHORT-CIRCUIT REGIM ($I_t = 40$ kA, RMS value)

	Conductor 1	Conductor 2	Conductor 3	Shield
Joule heat (average value) [kW/m]	21.918	21.918	21.918	25.689
	20.744 *	20.744 *	20.744 *	4.752 *
Joule heat without shield (average value) [kW/m]	23.655	23.655	23.655	-
Total current (peak value) [kA]	56.568	56.568	56.568	$0.1849 \ 10^{-3}$
Electrodynamic forces (average value) [N/m]	1180.9	1180.8	1180.9	0.47149
	616.64 *	616.42 *	616.61 *	0.063 *
x – component [N/m]	1166.4	-742.93	-423.69	-0.197
	615.6 *	-338.53 *	-277.32 *	0.0626 *
y – component [N/m]	-184.91	-917.74	1102.3	-0.42798
	-35.84 *	-515.14 *	550.74 *	0.0102 *
Oscilating component [N/m]	1498.9	1499	1498.9	146.21
	890.65 *	890.57 *	890.57 *	325.61 *
Electrodynamic forces without shield (average value) [N/m]	1230.8	1230.9	1231	-
x – component [N/m]	1229.8	-657.68	-572.5	-
y – component [N/m]	-49.299	-1040.4	1089.8	-
Error for electrodynamic force with shield and non shield [%]	4.22	4.24	4.24	-
Oscilating component	1589.5	1589.5	1589.6	-
Skin effect coefficient ($k_s = R_{AC}/R_{DC}$)	1.201	1.201	1.201	-
Voltage drop [V/m]	5.6477	5.6476	5.6476	$2.1285 \ 10^{-5}$
	4.964 *	4.964 *	4.964 *	$0.735 \ 10^{-5}$ *

TABLE III. TEMPERATURES OF CONDUCTOR AND SHIELD AT RATED CURRENT

Temperature	Analytical	QuickField
Conductor, θ_1 [^{o}C]	75.89	66.13
	71.21 *	65.58 *
Shield, θ_2 [^{o}C]	52.75	47.25
	49.5 *	41.76 *

TABLE IV. TEMPERATURE EVOLUTION AT SHORT-CIRCUIT

Temperature [^{o}C]	Time [s]			
	1	*5*	*10*	*20*
conductor	66.15	85.36	108.43	149.61
	70.07 *	86.62 *		
shield	42.27	46.63	47.64	58.73
	41.77 *	42.2 *		

IV. CONCLUSIONS

The QuickField model in rated and short-circuit regimes allows the following facilities:

- determination of the losses in conductors and shield (by Joule effect and eddy currents);
- determination of the temperature distribution in busbar system with common shield;
- determination of physical quantities such as resistance in AC, inductance and impedance of each conductor, magnetic energy, voltage drop, skin effect coefficient etc.
- determination of electrodynamic forces that occur between active conductors;

For the aluminum shield is obtained a significant reduction of the electrodynamic forces acting between conductors (about 50%) than for the iron shield.

The losses in shield at rated and short circuit regimes are smaller by 80% for aluminum than iron.

The losses in conductors are smaller by 10% for aluminum than iron at rated current and by 5-6% in short-circuit regime.

The developed model can also be coupled to a stress analysis module to determination of mechanical stress in the encapsulated bars system.

To increase the accuracy of the results, all the influences on the heat transfer coefficient (emissivity, temperature, temperature variation of the physical properties of air) should be taken into consideration.

The numerical model can be used to design and optimize the geometry of busbars system with common shield.

REFERENCES

[1] I. Popa, M. Ciontu, A. I. Dolan, "QuickField Analysis of a Three-Phase Encapsulated Busbars System," Annals of the University of Craiova, Year 37, No. 37, 2013, pp. 22-28.

[2] I. Popa, A. I. Dolan, "Thermal Modeling and Experimental Validation of an Encapsulated Busabars System," XVIII-the International Symposium on Electrical Apparatus and Technologies SIELA 2014, 29-31 May 2014, Bourgas, Bulgaria, Proceeding of Digest, pp. 105-106.

[3] H-K. Kim, Y-H Oh, S-H Lee, "Calculation of Temperature Rise in Gas Insulated Busbar by Coupled Magneto-Thermal-Fluid Analysis," Journal of Electr. Eng. & Tech. Vol. 4, No. 4, pp. 510-514, 2009.

[4] R. Coneybeer, M. Marietta, W. Z. Black, G. Woodruff, R. A. Bush, "Steady-State and Transient Ampacity of Bus Bar," IEEE Trans. on Power Delivery. Vol. 9, No. 4, October 1994, pp. 1822-1829.

[5] J. K. Kim, S. C. Hahn, K. Y. Park, H. K. Kim, Y. H. Oh, "Temperature Rise Prediction of EHV GIS Bus Bar by Coupled Magnetothermal Finite Element Method," IEEE Transactions on Magnetics. Vol. 41, No. 5, May 2005, pp. 1636-1639.

[6] J. K. Kim, J-Y. Lee, S-B. Wee, S-C Hahn, "A Novel Coupled Magneto-Thermal-Flow Analysis for Temperature Rise Prediction of Power Apparatus," Proceedings of International Conference on Electrical Machines and Systems, 2008 - ICEMS 2008, pp. 585-588.

[7] Gh. Hortopan, Electrical Apparatus, Vol. 1 – Principles, Tehnica Edition, Bucharest, 2000 (in Roumanian).

[8] Emanuel, A., Doepken, H. C. "Calculation of Losses in Steel Enclosures of Three Pase Bus or Cables," IEEE Transaction on PAS, vol. 93, 1974, No. 6, pp. 1758-1767.

[9] Doepken, H. C. Jr. "Calculated Heat Transfer Characteristics of Air and SF_6", IEEE Transaction on PAS, vol. 89, No. 8, 1970, pp. 1979-1985.

[10] *** Tera Analysis Ltd. QuickField Software version 5.10 Professional and User Manual. http://www.quickfield.com, 2014.

[11] F.J. McQuillan, J.R. Culham and M. M. Yovanovich "Properties of Dry Air at One Atmosphere," Microelectronics Heat Transfer Laboratory Report UW/MHTL 8406 G-01, 1984, http://www.mhtlab.uwaterloo.ca/pdf_reports/mhtl_G01.pdf

[12] V. Hatziathanassiou, D. Labridis, "Coupled Magneto-Thermal Field Computation in Three-Phase Gas Insulated Cables. Part 1: Finite Element Formulation," Archiv fur Elektrotechnik 76 (1993), pp. 285-292.

[13] S. W. Kim. H. H. Kim, S. C. Hahn, B. Y. Lee, K. Y. Park, Y. J. Shin, W. P. Song, J. B. Kim and I. H. Shin, "Coupled Finite-Element-Analytic Technique for Prediction of Temperature Rise in Power Apparatus," IEEE Transaction on Magnetics, vol. 38, No. 2, March 2002, pp. 921–924.

[14] I. Popa, A. I. Dolan, "Magneto-Thermal Modeling of an Encapsulated Busbars System with Common Shield," ICATE 2014 - International Conference on Applied and Theoretical Electricity, 23-25 October 2014, Craiova, Romania, Proceedings of Full Papers, paper 4.3, IEEE Catalog No. CFP1499S-USB, ISBN: 978-1-4799-4162-9.

[15] Gh. Hortopan, I. O. Vlase, S. Nițu, Ecranarea electromagnetică în tehnica curenților intenşi – in roumanian, (Electromagnetic Shielding in High Currents Technique), Editura Tehnică, Bucureşti, 1990.